Investigation of the Achaemenid period pottery production technology from the Seyitömer Mound (Kütahya, Turkey)

A. İssi[1], C. Serkaya[1], V. Uz[1] & A. N. Bilgen[2]
[1]*Department of Materials Science and Engineering, Dumlupınar University, Turkey*
[2]*Department of Archaeology, Dumlupınar University, Turkey*

Abstract

There are many archaeological excavations still being performed in Anatolia to unearth the cultural heritages from the past civilizations. Archaeological excavations started in the Seyitömer Mound in 1989. It is located on a large coal reserve and archaeological excavations need to be completed as soon as possible to utilize the mine. Pottery sherds investigated in this study were unearthed in the Seyitömer Mound and they belong to the Achaemenid period. Characterization studies on findings may contribute to archaeological knowledge about how they produced artifacts. To study the production technology of the Achaemenid pottery sherds, chemical analysis of samples was performed by wavelength dispersive X-ray fluorescence (WDXRF) and mineralogical/phase composition analysis was performed by X-ray diffraction (XRD). Scanning electron microscopy (SEM) and microanalysis technique (EDX) were performed for microstructural and microchemical analysis. Thermogravimetric–differential thermal analysis (TG–DTA) were employed to characterize the potsherds. It may be concluded from the results that ceramic bodies have been produced from illitic clays rich in iron and magnesium, containing carbonated minerals such as calcite and dolomite. Finally, considering the obtained results, firing temperatures of the potsherds could be between 600°C and 900°C.

Keywords: Seyitömer Mound, Achaemenid period, ceramic artifact, characterization, archaeometry.

WIT Transactions on The Built Environment, Vol 168, © 2015 WIT Press
www.witpress.com, ISSN 1743-3509 (on-line)
doi:10.2495/SD150531

1 Introduction

There are several ancient sites belonging to many civilizations lived in Anatolia in different periods of history. Archaeological excavations are still being carried out to unearth the cultural heritage of the past civilizations. One of them is the Seyitömer Mound. The Seyitömer Mound is located 25 km northwest of the centre of Kütahya province. The Mound is 150x140 m in size and has a height of 23.5 m. In order to receive 12 million tonnes of coal reserve under the mound, archaeological excavations are being held in the archaeological site. The archaeological excavations were started in 1989. It has been found that the Seyitömer Mound was inhibited by civilizations in the Bronze Age, Achaemenid, Hellenistic and Roman periods (Bilgen [1]). Archaeometrical studies gather different branches of science such as materials science, physics, chemistry and others. Archaeological ceramics may be investigated with different characterization techniques to enlighten production technology of the wares (Papachristodoulou *et al.* [2], Barone *et al.* [3]).

Thirty pottery sherds unearthed in the Seyitömer Mound belonging to the Achaemenid period have been investigated. Chemical analysis of samples was performed by wavelength dispersive X-ray fluorescence (WDXRF) and mineralogical/phase composition analysis was performed by X-ray diffraction (XRD) (Vinagre *et al.* [4], Demirel *et al.* [5], Kennett *et al.* [6]) to perform archaeometrical characterization of the artifacts. Scanning electron microscopy (SEM) and energy dispersive spectroscopy (EDS) were used for identification of microstructural and microchemical properties of the samples. Thermogravimetric–differential thermal analysis (TG–DTA) was performed to observe the thermal behaviours of the samples to predict the maximum firing temperatures.

Figure 1: A photograph and a map showing the location of the Seyitömer Mound.

2 Materials and methods

The representative photos of the Achaemenid period samples coded as A10, A11, A14 and A29 are given in Figure 2.

Figure 2: Photos of A10, A11, A14 and A29 coded samples.

Samples were cut by diamond cutting discs and 0.8–1.5 g of samples were obtained. Samples were stored in deionized water to remove impurities for 2 days. Cleaned samples were dried at room temperature. Fine powders were prepared in an agate mortar in order to be analysed by WDXRF and XRD techniques. A Rigaku Miniflex powder diffractometer with Cu Kα radiation (λ= 1.5418 Å) was used for the mineralogical analysis. XRD patterns were obtained by scanning 5° to 55° in 2θ, with a goniometer speed of 2°/min, operating at 40 kV and 30 mA. The interpretation of mineralogical content of the data was conducted with JADE 7 software by searching and matching the powder diffraction files. A Rigaku ZSX primus wavelength dispersive X-ray fluorescence (WDXRF) instrument was used for chemical analysis of the elements. The measurements were carried out on glass tablets prepared by fluxing powdered samples with $Li_2B_4O_7$ in 1:10 weigh ratio. The calculation of the semi-quantitative results was conducted with ZSX software. The results were given as oxides. The microstructural and microchemical aspects of the representative potsherds were investigated using FEI Nova Nano 650 SEM instrument which also includes an EDS detector. Setaram Labsys Evo instrument was used for TG–DTA analysis. A heating rate of 10°C/min was performed in oxidative atmosphere from room temperature to 1200°C.

3 Results and discussions

3.1 Chemical analysis result and discussion

Instead of giving all the results of the study, chemical analysis results belonging to A10, A11, A14 and A29 which are calcium poor and rich and representing chemical analysis of ceramic groups were given in Table 1.

As seen from the results, the maximum percentage of CaO belongs to the A11 coded sample, the minimum percentage belongs to the A29 coded sample. Considering the total of alkaline and alkaline-earth oxides, A11 have the maximum quantity.

Table 1: Chemical analysis results of A10, A11, A14 and A29. The term of "n.d." indicates not detected or under the limits of detection by WDXRF technique performed.

	Calcium Rich		Calcium Poor	
Oxide	**A11**	**A14**	**A10**	**A29**
Na_2O	0.4033	0.4169	2.117	0.586
MgO	3.0006	5.9993	2.2023	1.3813
Al_2O_3	15.5556	12.1807	15.6316	22.0702
SiO_2	48.3133	56.5772	67.4659	59.8809
P_2O_5	0.2114	0.1511	0.2873	0.3258
SO_3	0.0741	0.0399	0.0568	0.238
As_2O_3	0.0306	n.d.	0.0128	0.0158
K_2O	2.2499	2.785	4.1811	4.9322
CaO	19.9717	12.4227	1.5857	1.5585
TiO_2	1.1477	0.7191	0.6752	0.8538
TeO_2	n.d.	n.d.	n.d.	n.d.
Cr_2O_3	0.1035	0.2366	0.0851	0.1088
MnO	0.1903	0.1245	0.0506	0.1427
Fe_2O_3	8.6427	8.192	5.2697	7.7677
Co_2O_3	n.d.	0.0104	n.d.	n.d.
NiO	0.0327	0.0876	0.0275	0.0234
CuO	0.0159	n.d.	n.d.	0.0205
ZnO	0.0182	0.0212	0.0112	0.0307
Rb_2O	n.d.	n.d.	0.0351	n.d.
SrO	0.0145	0.0175	0.0183	0.0129
ZrO_2	0.024	0.0184	0.0307	0.0507
BaO	n.d.	n.d.	0.256	n.d.
SnO_2	n.d.	n.d.	n.d.	n.d.
Nb_2O_5	n.d.	n.d.	n.d.	n.d.
Ag_2O	n.d.	n.d.	n.d.	n.d.
PbO	n.d.	n.d.	n.d.	n.d.
Cl	n.d.	n.d.	n.d.	n.d.
ThO_2	n.d.	n.d.	n.d.	n.d.
V_2O_5	n.d.	n.d.	n.d.	n.d.

3.2 Mineralogical/phase analysis results and discussion

Determined minerals/phases for the samples are: Quartz (SiO_2), Plagioclase, Illite ($(K,H_3O)Al_2Si_3AlO_{10}(OH)_2$), Microcline ($KAlSi_3O_8$), Calcite ($CaCO_3$), Muscovite ($KAl_2(Si_3Al)O_{10}(OH,F)_2$), Gehlenite ($Ca_2Al_2SiO_7$), Dolomite ($CaMg(CO_3)_2$), Hematite ($Fe_2O_3$), Maghemit ($Fe_20_3$), Kaliophilite ($KAlSiO_4$), Wollastonite ($CaSiO_3$), Diopside ($Ca(Mg,Al)(Si,Al)_2O_6$). XRD analysis results of A10, A11, A14 and A29 coded samples and raw materials of clays are given in Table 2.

Table 2: XRD analysis results of A10, A11, A14 and A29 coded samples and raw materials of clays.

Sample Code	Minerals/Phases
A10	Quartz, Plagioclase, Muscovite, Microcline, Wollastonite, Gehlenite, Maghemite.
A11	Quartz, Plagioclase, Kaliophilite, Calcite, Dolomite, Hematite, Maghemite.
A14	Quartz, Plagioclase, Muscovite, Calcite, Dolomite, Maghemite.
A29	Quartz, Plagioclase, Muscovite, Microcline, Kaliophilite, Diopside, Gehlenite, Maghemite.
SNLKKY	Quartz, Plagioclase, Illite/Muscovite, Montmorillonite, Kaolinite, Calcite, Dolomite.
AYVALIB	Quartz, Plagioclase, Illite/Muscovite, Talc, Kaolinite, Kaliophilite, Calcite, Dolomite.
CKOY2B	Quartz, Plagioclase, Illite/Muscovite, Kaolinite/Montmorillonite, Calcite.
IK3A	Quartz, Plagioclase, Illite/Muscovite, Talc, Montmorillonite, Kaolinite, Calcite.
SO1K	Quartz, Plagioclase, Illite/Muscovite, Montmorillonite, Kaolinite, Calcite, Dolomite.

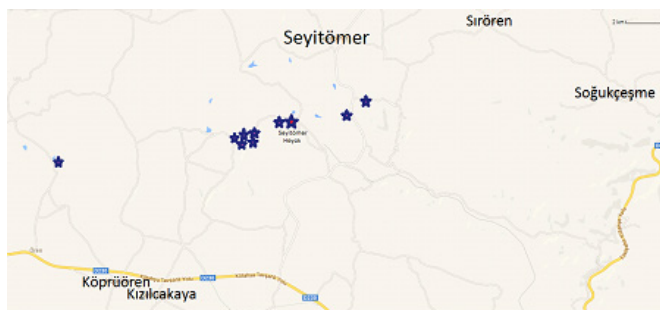

Figure 3: A map shows the raw materials (clays) collected around the Seyitömer Mound.

XRD results of the raw materials (clays) collected around the Seyitömer Mound are also given in Table 2. They were coded as SNLKKY, AYVALIB, CKOY2B, IK3A and SO1K.

Quartz is a mineral with high heat of melting. For this reason, quartz mineral exists in all samples. Quartz and feldspars can persist up to 1000°C (İssi *et al.* [7]). Gehlenite begins to form at 800°C and disappear at 900°C (Veniale [8]). Illite/muscovite or mica structure breaks down in the range of 900–1000°C (Grimshaw [9]). Gehlenite may be formed at 850°C with the reaction of CaO and illite structure, diopside may be generated from dolomite and silica reactions at 800–900°C (Cultrone *et al.* [10]).

A10, A14 and A29 coded samples contain illite/muscovite minerals. They could have been fired under 1000°C. A10 and A29 coded samples contains gehlenite mineral. A10 and A29 coded samples possibly sintered around 800°C. Calcite and dolomite decomposition begin under 700°C and is completed up to 850°C (Lopez-Arce *et al.* [11]). Therefore, A11 and A14 coded samples could have been fired in the lowest temperature. Another suggestion from the results is related with the atmosphere of firing. Hematite indicates oxidative firing (Damjanovic *et al.* [12]). However, existence of maghemite phase on XRD pattern cannot be excluded but, reductive atmosphere should have been provided for firing (Legodi and de Waala [13]). A29 coded sample contains diopside. Presence of diopside indicates that the original raw material had dolomite or another type of mineral which contain magnesium. In the case of dolomite presence, diopside is originated through the following reaction beginning at 900°C. It may be suggested that A29 coded sample firing temperature is around 900°C (Fort *et al.* [14]).

3.3 SEM analysis results and discussion

SEM images of Ca rich and poor samples are given in Figure 4.

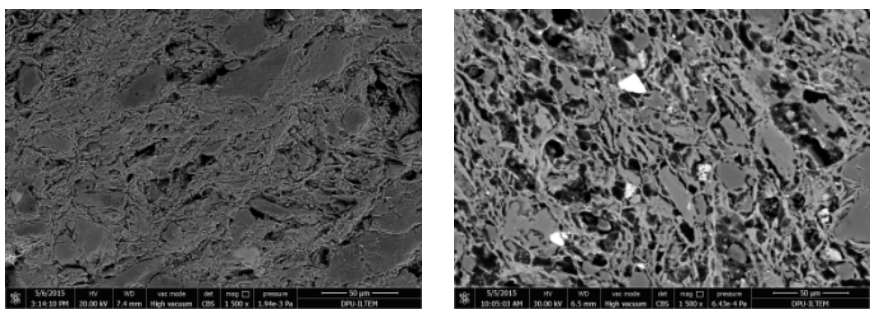

(a) (b)

Figure 4: SEM images of Ca rich A11 coded sample (a) and Ca poor A29 coded sample (b).

Some changes with increasing temperature in clay based ceramics can be described as (i) interactions between clay matrix and grains, (ii) shape changes of grains, (iii) increase of the aggregation rate within the clay matrix with the

formation of secondary porosity, and (iv) formation of intergranular bridges. These changes become more evident in calcareous clays than the siliceous materials including clays (Riccardi *et al.* [15]). Since some of the samples contain high amounts of calcium, SEM images exhibited predominantly arrangements of calcium rich new mineral formations in the microstructure of the samples (Figure 4(a)). Quartz is one of the primary components of clay based ceramics with high melting temperature. It is considered that quartz is relatively insoluble below 1250°C, dissolution of quartz forms silica-rich amorphous solution rims around quartz grains (Iqbal and Lee [16]). Quartz grain dissolution into vitrified clay matrix of the sample may easily be distinguished by the atomic contrast difference in BSE images. Feldspar is believed to melt around 1100°C in the contact zone between feldspar crystals and clay relicts and potash matrix require high temperature around 1200°C.

3.4 Thermogravimetric–differential thermal analysis TG-DTA results and discussion

TG–DTA is the preferred method in characterization of potteries. This technique allows the examination of changes occurred due to the decomposition, transformation and formation reactions during a controlled heating process (Drebushchak *et al.* [17]). Samples were heated from room temperature to 1200°C with a heating rate of 10°C/min in order to expose the enthalpy changes (plotted by DTA curves with endothermic and exothermic effects) and weight loss/gain (plotted by TG curves).

The endothermic effect from room temperature to 200°C is due to the release of hygroscopic water (Maritan *et al.* [18]). At higher temperatures of 200–300°C the endothermic effect depicts the removal of the chemically bound water, but it may not met in the present study (Paama *et al.* [19]). Depending on the area of the peaks observed in the range of 200–650°C, the exothermic effect identified within these temperatures was attributed to the combustion of organic materials, not completely burnt during firing in reducing condition and transformed into carbonaceous particles which are thought to be deliberately added into the ceramic paste to increase its plasticity or were contained in the clay utilized in the manufacture (Palanivel and Rajesh Kumar [20]). The endothermic effects observed at 700–875°C indicated the decarbonation reactions of mainly calcite and dolomite (Meyvel *et al*. [21]).

TG–DTA results of selected samples are given in Figures 5 and 6.

Mass loss peak in A10 coded sample is around 5.5%. As it can be seen from the Figure 5, mass change is methodical up to 400°C. Considering TG analysis with XRD results weight loss originates from the reactions of unbound or adsorbed water or burning of organic substance. DTA analysis shows exothermic reaction in 435°C. This may suggest of organic based materials burning. Endothermic reaction in 575°C is also due to the crystal water decomposition in A10 coded sample. Mass loss of A11 coded sample is around 7%. According to TG analysis mass change is methodical up to 640°C and considering with XRD results,

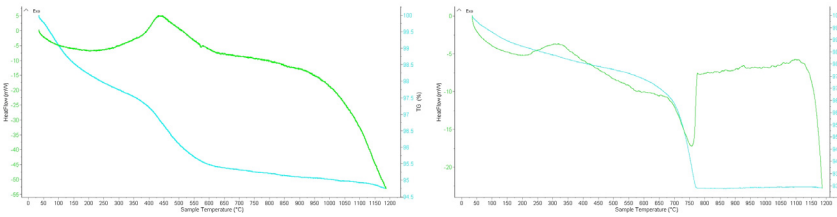

(a) (b)

Figure 5: TG–DTA curve of the sample of A10 (a) & A11 (b).

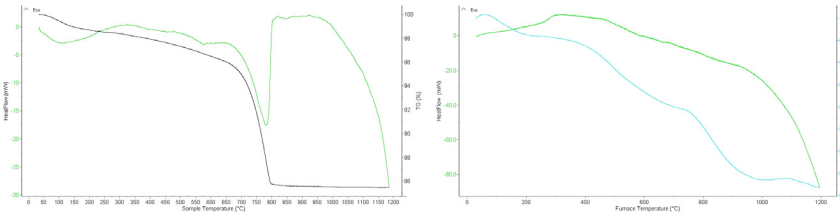

(a) (b)

Figure 6: TG–DTA curve of the sample of A14 (a) and A29 (b).

conclusions are similar with A10 coded sample. DTA analysis of A11 coded sample shows a reaction in 725°C. This may suggest calcite decomposition. Mass loss of A14 coded sample is around 14%. Mass change is methodical up to 675°C. DTA analysis of A14 coded sample shows endothermic reaction in 575°C. This may be crystal water decomposition. Endothermic reaction at 780°C also because of calcite decomposition. Mass loss of A29 coded sample is around 4%. As seen in Figure 6 mass change is methodical up to 775°C. DTA analysis shows there are no materials such as clays or silicates to make any weight loss or endo-exothermic reactions.

4 Conclusions

From WDXRF, XRD, SEM and TG–DTA analysis results obtained, the Achaemenid period ceramics unearthed in the Seyitömer Mound have been produced from clay deposits containing illitic type minerals with rich in iron and calcium rich and poor accessory minerals. To compare with regional geological formations and raw material sources, it may be suggested that local raw material source is enough to produce such kind of ceramic wares during the Achaemenid period. According to phases/minerals in Achaemenid period samples firing temperatures are between 600°C and 900°C.

Acknowledgement

This study is a part of ongoing project titled "Archaeometrical Characterization of Ceramic Findings Belonging to Achaemenid, Hellenistic and Roman Periods from Seyitömer Mound (Kütahya)" with the project number of 113K096. The Scientific and Technological Research Council of Turkey (TÜBİTAK) is acknowledged.

References

[1] Bilgen A.N., Seyitömer Höyük Kazısı Ön Raporu. P.1 Kütahya, 2011 (in Turkish).
[2] Papachristodoulou C., Oikonomou A., Ioaniddes K. & Gravani K., A Study of Ancient Pottery by Means of X-Ray Fluorescence Spectroscopy, Multivariate Statistics and Mineralogical Analysis. Analytica Chimica Acta., 573, pp. 347-353, 2006.
[3] Barone G., Crupi V., Galli S., Majolino D., Migliardo P. & Venuti V., Spectroscopic İnvestigation of Greek Ceramic Artefacts. Journal of Molecular Structure, 651, pp. 449-458, 2003.
[4] Vinagre U.M., Latini R.M., Bellido A.V.B., Buarque A. & Borges A.M., Ancient Ceramics Analysis by Neutron Activation in Association with Multivare Methods, Brazilian Journal of Physics, 35, pp. 779-781, 2005.
[5] Demirel M., Sevin F.B., Say R. & Yazan Y., Propranolol HCl Imprinted Polymeric Microspheres: Development, Characterization and Dissolution. FABAD J. Pharm. Sci., 32, pp. 147-157, Ankara, 2007.
[6] Kennett D.J., Sakai S., Neff H., Gossett R. & Larson D.O., Compositional Characterisation of Prehistoric Ceramics: A New Approach. Journal of Archaeological Science, 29, pp. 443-455, 2002.
[7] İssi A., Kara A. & Alp A.O., An Investigation of Hellenistic Period Pottery Production Technology from Harabezikan/Turkey. Ceramics International, 37, pp. 2575-2582, Eskişehir, 2011.
[8] Veniale F., Modern techniques of analysis applied to ancient ceramics. In: Advanced workshop on analytical methodologies for the investigation of damaged Stones, Pavia, (Italy), 1990.
[9] Grimshaw R.W., The Chemistry and Physics of Clays. Techbooks, p. 727, India, 1971.
[10] Cultrone G., Navarro C.R., Sebastian E., Cazalla O. & Torre M.J., Carbonate and Silicate Phase Reactions during Ceramic Firing. Eur. J. Mineral., 13, pp. 621-634, Stuttgart (Germany), 2001.
[11] López-Arce P., Garcia-Guinea J., Gracia M. & Obis J., Bricks in historical buildings of Toledo City: characterisation and restoration. Mater. Charact., 50, pp. 59-68, 2003.
[12] Damjanovic L., Antunovic I.H., Mioc U.B., Bikic V., Milanovic D. & Evans I.R., Archaeometric study of medieval pottery excavated at Stari (Old) Ras Serbia. J. Archaeol. Sci., 38, pp. 818-828, 2011.

[13] Legodi M.A. & de Waala M.A., The preparation of magnetite, goethite, hematite and maghemite of pigment quality from mill scale iron waste. Department of Chemistry, University of Pretoria, v.74, i.1, pp. 161-168, Pretoria (South Africa), 2007.
[14] Fort R., Alvarez de Buergo M., Gomez-Heras M. & Vazquez-Calvo C., Heritage, Weathering and Conservation. Taylor & Francis Group, Vol. 2, p. 940, London, 2006.
[15] Riccardi M.P., Messiga B. & Duminuco P., An approach to the dynamics of clay firing, Appl. Clay Sci., 15, pp. 393-409, 1999.
[16] Iqbal Y. & Lee W.E., Microstructural evolution in triaxial porcelain, J. Am. Ceram. Soc., 83, pp. 3121-3127, 2000.
[17] Drebushchak V.A., Mylnikova L.N., Drebushchak T.N. & Boldyrev V.V., The investigations of ancient pottery, J. Therm. Anal. Calorim., 82, pp. 617-626 2005.
[18] Maritan L., Nodari L., Mazzoli C., Milano A. & Russo U., Influence of firing conditions on ceramic products: experimental study on clay rich in organic matter. Appl. Clay Sci., pp. 311-315, 2006.
[19] Paama L., Pitkanen I. & Peramaki P., Analysis of archeological samples and local clays using ICP-AES, TGDTG and FTIR techniques. Talanta, 51, pp. 349-357, 2000.
[20] Palanivel R. & Rajesh Kumar U., Thermal and spectroscopic analysis of ancient potteries. Rom. J. Phys., 56, pp. 195-208, 2011.
[21] Meyvel S., Sathya P. & Velraj G., Thermal characterization of archaeological potsherds recently excavated in Nedunkur, Tamilnadu, India, Cerâmica, 58 pp. 338-341, 2012.